Novel *p*-Phenylenevinylene Compounds Containing Thiophene or Anthracene Moieties and Cyano−Vinylene Bonds for Photovoltaic Applications

John A. Mikroyannidis,*,† Minas M. Stylianakis,† P. Balraju,‡ P. Suresh,‡ and G. D. Sharma*,‡

Chemical Technology Laboratory, Department of Chemistry, University of Patras, GR-26500 Patras, Greece, and Physics Department, Molecular Electronic and Optoelectronic Device Laboratory, JNV University, Jodhpur 342005, India

ABSTRACT Two novel soluble compounds **T** and **A** that contain a central dihexyloxy-*p*-phenylenevinylene unit, intermediate moieties of thiophene or anthracene, respectively, and terminal cyano−vinylene nitrophenyls were synthesized and characterized. They showed moderate thermal stability and relatively low glass transition temperatures. These compounds displayed similar optical properties. Their absorption was broad and extended up to about 750 nm with the longer-wavelength maximum around 640 nm and an optical band gap of ~1.70 eV. From the current−voltage characteristics of the devices using both compounds **T** and **A**, it was concluded that both compounds behave as p-type organic semiconductors with hole mobility on the order of 10^{-5} $cm^2/(V\ s)$. The power conversion efficiency (PCE) of the devices based on these compounds was 0.019% and 0.013% for compounds **A** and **T**, respectively. When compounds **A** and **T** were blended with [6,6]-phenyl-C61-butyric acid methyl ester (PCBM), the PCE dramatically increased up to 1.66% and 1.36% for devices with **A**:PCBM and **T**:PCBM, respectively. The efficiencies of the devices were further enhanced upon thermal annealing up to 2.49% and 2.33% for devices based on **A**:PCBM and **T**:PCBM, respectively.

KEYWORDS: *p*-phenylenevinylene • thiophene • anthracene • cyano−vinylene • photophysics • small-molecule solar cell • organic solar cells

INTRODUCTION

There is great interest in developing efficient plastic photovoltaic (PV) devices as a low-cost alternative to conventional inorganic solar cells (1). In contrast to the inorganic counterparts, an organic/polymeric π-conjugated semiconducting materials-based PV device often suffers from low energy conversion efficiencies because of poor photoinitiated charge transfer/dissociation and transport of photogenerated charges. It has been shown that the heterojunction interfaces in a donor−acceptor composite can provide efficient photogenerated charge dissociation and the created charges can efficiently be transported separately by the donor and acceptor to the opposite electrodes (2). Much effort has recently concentrated on the bulk heterojunction (BHJ) approach in which the active layer is based on the interpenetrating composite of donor and acceptor molecules/polymers because of its ease of fabrication and high efficiency (3). The power conversion efficiencies (PCEs) of a BHJ PV cell based on a regioregular poly(3-hexylthiophene) (P3HT) as an electron-donating (p-type) material blended with a soluble [6,6]-phenyl-C61-butyric acid methyl ester (PCBM) as an electron-accepting (n-type) material have reached greater than 5% through control of the nanostructure formation of an interpenetrating donor/acceptor polymer network (4).

Poly(dialkoxy-*p*-phenylenevinylene)s (PPVs) and its derivatives are attractive in conjugated polymers because alkoxy substitutions at the 2,5-hydrogens of the phenyls make them possess remarkable properties such as solubility and processability (5). It is a general trend that the band gaps of PPV derivatives are reduced as electron-donating alkoxy groups attached to the phenylene rings of PPV, and then the wavelength of the emitted light is red-shifted, so most of the PPVs show emissions in the red-orange region (6−8). An example of promising organic solar cells is that based on poly[2-methoxy-5-(2′-ethylhexyloxy)-1,4-phenylenevinylene] and a [6,6]-phenyl-C60-butyric acid methyl ester heterojunction (MEH-PPV/PCBM), which was prepared and experimentally studied earlier. The cell showed 2.9% PCE under 100 mW/cm^2 illumination intensity, as reported by Nunzia et al. (9) and by others (10). Li et al. reported lower conversion efficiency for similar cells based on MEH-PPV and polymers with substituents containing C60 moieties (11). Because of its special features and applicability in PV devices, MEH-PPV has been heavily studied from different points of view, namely, carrier mobility (12), the ability to sensitize titania (13), LED devices (14), luminescence (15−20) and other characteristics. This interest reflects the future expectations from the MEH-PPV/PCBM organic solar cell.

* Corresponding authors. Tel: +30 2610 997115 (J.A.M.), 91-0291-2720857 (G.D.S.). Fax: +30 2610 997118 (J.A.M.), 91-0291-2720856 (G.D.S.). E-mail: mikroyan@chemistry.upatras.gr (J.A.M.), sharmagd_in@yahoo.com (G.D.S.).
Received for review April 21, 2009 and accepted July 6, 2009
† University of Patras.
‡ JNV University.
DOI: 10.1021/am900270s

To obtain a panchromatic absorption band, the π-conjugated system of the sensitizing molecules should be expanded. Introduction of electron-donating and -withdrawing groups to the conjugated structure gives the charge-transfer character of absorption and wide and high absorptivity. Cyano groups could be used as the electron-withdrawing units. The introduction of cyano groups onto a poly(*p*-phenylenevinylene) backbone has been proven as an effective way of lowering the lowest unoccupied molecular orbital (LUMO) level of the polymer (21). Furthermore, the electrochemical stability of the polymers could be enhanced by introducing cyano groups (22), which is also desirable for optoelectronic devices. An n-type conjugated poly(1,8-dioctyloxy-*p*-2,5-dicyanophenylene) has recently been prepared through Stille coupling (23). On the other hand, the photocurrents that can be attained in PV cells have been enhanced by attaching electron acceptors such as a nitro group to the polythiophene chain (24, 25). Direct conjugation of the electron-withdrawing nitro group with the poly(terthiophene) backbone because of the presence of an alkene linker (26, 27) can facilitate charge separation of excitons formed when the photoelectrochemical cell is exposed to light (24). Recently, certain nitro-containing materials have been synthesized and used for PV cells (28−31). Finally, anthracene-containing compounds have been used for BHJ solar cells. Particularly, a diarylanthracene bearing two dihexyloxy-substituted benzene rings has been synthesized and used as donor for BHJ solar cells with PCBM (32). Anthracene-containing phenylene− or thienylene−vinylene copolymers have been synthesized in our laboratory and used for PV cells very recently (33).

To date, there has not been much success in solution processing of small molecules for organic PVs (OPVs) despite their advantages over polymeric semiconductors, which include monodispersity, high charge carrier mobility, and relatively simple synthesis (34). It is generally believed that factors such as limited solubility and a tendency to aggregate in most organic solvents are responsible for the difficulty in solution processing of small molecules. Strong intermolecular forces between conjugated small molecules facilitate intermolecular electron delocalization, which is desirable for efficient charge transport. In addition, crystallization of solution-cast small molecules on a substrate often results in poor film formation with polycrystalline domains, which are characterized by unfavorable grain connectivity and suboptimal crystalline ordering (34). Solution-processed small molecules, which have been used for PV cells, have recently been reviewed (34). Efficient BHJ PV solar cells based on symmetrical D-π-A-π-D organic dye molecules (35), squaraine (36, 37), phthalocyanines (38, 39), oligothiophene with dialkylated diketopyrrolopyrrole (40, 41), 2-vinyl-4,5-dicyanoimidazole (Vinazene) (42, 43) and star-shaped molecules have very recently been reported (44−48). The highest PCE reported to date for solar cells using solution-processable small molecules is 3.0% (40).

The present investigation describes the synthesis and characterization of two compounds that contain central *p*-phenylenevinylene unit, intermediate thiophene or anthracene moieties, and terminal cyano−vinylene nitrophenyls. They were prepared by a simple two-step synthetic route and carried solubilizing dihexyloxy side groups on the phenylene central unit. They possess the donor−acceptor (D−A) architecture. Specifically, their central dialkoxyphenylene and intermediate thiophene or anthracene behaved as electron-donating segments, while the terminal cyano−vinylene nitrophenyls acted as electron acceptors. Thus, an intramolecular charge transfer took place in these compounds, which reduced their optical band gaps. The present study revealed that these compounds had potential applications for PV cells. The current−voltage ($J-V$) characteristics of the devices based on both compound **A** and **T** reveal that these are p-type organic semiconductor. The PCEs of the PV devices based on blends with PCBM are about 1.66% and 1.36% for **A** and **T**, respectively, which are further improved up to 2.49% and 2.33% upon thermal annealing.

EXPERIMENTAL SECTION

Characterization Methods. IR spectra were recorded on a Perkin-Elmer 16PC FT-IR spectrometer with KBr pellets. ^{1}H NMR (400 MHz) spectra were obtained using a Brucker spectrometer. Chemical shifts (δ values) are given in parts per million with tetramethylsilane as an internal standard. UV−vis spectra were recorded on a Beckman DU-640 spectrometer with spectrograde tetrahydrofuran. Thermogravimetric analysis (TGA) was performed on a DuPont 990 thermal analyzer system. Ground samples of about 10 mg each were examined by TGA, and weight loss comparisons were made between comparable specimens. Dynamic TGA measurements were made at a heating rate of 20 °C/min in an atmosphere of N_2 at a flow rate of 60 cm^3/min. Thermomechanical analysis (TMA) was recorded on a DuPont 943 thermomechanical analyzer using a loaded penetration probe at a scan rate of 20 °C/min in N_2 at a flow rate of 60 cm^3/min. The TMA experiments were conducted at least in duplicate to ensure the accuracy of the results. The TMA specimens were pellets of 10 mm diameter and ~1 mm thickness prepared by pressing powder samples for 3 min under 8 kp/cm^2 at ambient temperature. T_g is assigned by the first inflection point in the TMA curve, and it was obtained from the onset temperature of this transition during the second heating. Elemental analyses were carried out with a Carlo Erba model EA1108 analyzer.

Reagents and Solvents. 1,4-Divinyl-2,5-bis(hexyloxy)benzene (**1**) was prepared by a Stille coupling reaction (49) of 1,4-dibromo-2,5-bis(hexyloxy)benzene with tributylvinyltin (50). 9-Bromoanthracene-10-carbaldehyde (**2b**) was synthesized by brominating 9-anthracaldehyde in CH_2Cl_2 according to the reported method (33). 4-Nitrobenzyl cyanide (**4**) was synthesized from the nitration of benzyl cyanide with concentrated nitric and sulfuric acid (51). *N*,*N*-Dimethylformamide (DMF) and tetrahydrofuran (THF) were dried by distillation over CaH_2. Triethylamine was purified by distillation over KOH. All other reagents and solvents were commercially purchased and were used as supplied.

Preparation of Compounds. ***Compound* 3a.** A flask was charged with a mixture of **1** (0.1262 g, 0.381 mmol), 5-bromo-2-thiophenecarboxaldehyde (0.1459 g, 0.764 mmol), $Pd(OAc)_2$ (0.0017 g, 0.008 mmol), P(*o*-tolyl)$_3$ (0.0046 g, 0.151 mmol), DMF (4 mL), and triethylamine (5 mL). The flask was degassed and purged with N_2. The mixture was heated at 90 °C for 15 h under N_2. Then, it was filtered, and the filtrate was poured into methanol. Compound **3a** precipitated as an orange semisolid, which was isolated by decantation. The crude product was

purified by dissolution in THF and precipitation into methanol (0.15 g, 72%).

FT-IR (KBr, cm^{-1}): 3084, 2954, 2930, 2858, 1678, 1668, 1524, 1496, 1416, 1378, 1204, 1056, 976, 906, 866, 800.

^1H NMR ($CDCl_3$, ppm): 7.78 (s, 2H, CHO), 7.36 (m, 4H, olefinic), 7.21 (m, 4H, thiophene), 6.98 (m, 2H, phenylene), 3.95 (m, 4H, $OCH_2C_5H_{11}$), 1.79 (m, 4H, $OCH_2CH_2C_4H_9$); 1.34 (m, 12H, $OCH_2CH_2(CH_2)_3CH_3$), 0.91 (t, J = 6.9 Hz, 6H, $OCH_2CH_2(CH_2)_3CH_3$).

Anal. Calcd for $C_{32}H_{38}O_4S_2$: C, 69.78; H, 6.95. Found: C, 69.43; H, 6.87.

***Compound* 3b.** This compound was similarly prepared in 67% yield from the reaction of **1** with **2b**.

FT-IR (KBr, cm^{-1}): 3057, 2930, 2875, 2674, 2490, 1680, 1496, 1438, 1388, 1256, 1094, 1064, 964, 866.

^1H NMR ($CDCl_3$, ppm): 11.40 (s, 2H, CHO), 8.90−7.45 (m, 16H, anthracene), 7.25 (m, 4H, olefinic), 7.04 (m, 2H, phenylene), 3.94 (m, 4H, aliphatic $OCH_2C_5H_{11}$), 1.80 (m, 4H, aliphatic $OCH_2CH_2C_4H_9$), 1.33 (m, 12H, aliphatic $OCH_2CH_2(CH_2)_3CH_3$), 0.90 (t, J = 6.9 Hz, 6H, aliphatic $OCH_2CH_2(CH_2)_3CH_3$).

Anal. Calcd for $C_{52}H_{50}O_4$: C, 84.52; H, 6.82. Found: C, 84.10; H, 6.95.

***Compound* T.** A flask was charged with a solution of **3a** (0.34 g, 0.62 mmol) and **4** (0.20 g, 1.23 mmol) in anhydrous ethanol (20 mL). Sodium hydroxide (0.25 g, 6.16 mmol) dissolved in anhydrous ethanol (15 mL) was added portionwise to the stirred solution. The mixture was stirred for 1 h at room temperature under N_2 and then was concentrated under reduced pressure. Compound **T** precipitated as a dark-green solid by cooling into a refrigerator. It was filtered off, washed thoroughly with water, and dried (0.25 g, 54%).

FT-IR (KBr, cm^{-1}): 3080, 2952, 2924, 2866, 2154, 1606, 1524, 1448, 1346, 1288, 1106, 966.

^1H NMR ($CDCl_3$, ppm): 8.09 (m, 4H, aromatic ortho to nitro), 7.75 (s, 2H, olefinic of the cyano−vinylene bond); 7.57−7.48 (m, 4H, aromatic meta to nitro), 7.38 (m, 4H, other olefinic), 7.13−7.07 (m, 4H, thiophene), 6.96 (m, 2H, aromatic ortho to oxygen), 3.94 (m, 4H, aliphatic $OCH_2C_5H_{11}$), 1.80 (m, 4H, aliphatic $OCH_2CH_2C_4H_9$), 1.34 (m, 12H, $OCH_2CH_2(CH_2)_3CH_3$), 0.91 (t, J = 6.9 Hz, 6H, $OCH_2CH_2(CH_2)_3CH_3$).

Anal. Calcd for $C_{48}H_{46}N_4O_6S_2$: C, 68.71; H, 5.53; N, 6.68. Found: C, 68.42; H, 5.61; N, 6.63.

***Compound* A.** This compound was similarly prepared as a dark-green solid in 57% yield from the reaction of **3b** with **4**.

FT-IR (KBr, cm^{-1}): 3052, 2954, 2926, 2162, 1590, 1556, 1456, 1380, 1288, 1260, 1108, 969, 886, 754, 736.

^1H NMR ($CDCl_3$, ppm): 8.07−7.96 (m, 4H, aromatic ortho to nitro), 7.80 (s, 2H, olefinic of the cyano−vinylene bond), 7.60−7.44 (m, 20H, anthracene), 7.26 (m, 4H, other olefinic), 7.05 (m, 2H, aromatic ortho to oxygen), 3.94 (m, 4H, aliphatic $OCH_2C_5H_{11}$), 1.80 (m, 4H, aliphatic $OCH_2CH_2C_4H_9$), 1.33 (m, 12H, $OCH_2CH_2(CH_2)_3CH_3$), 0.90 (t, J = 6.9 Hz, 6H, $OCH_2CH_2(CH_2)_3CH_3$).

Anal. Calcd for $C_{68}H_{58}N_4O_6$: C, 79.51; H, 5.69; N, 5.45. Found: C, 79.23; H, 5.73; N, 5.49.

Electrochemical Characterization. The position of the LUMO and the highest occupied molecular orbital (HOMO) energy levels were estimated by cyclic voltammetry measurement. This was performed on an Autolab potentiostat PGSTAT-10, in an acetonitrile solution (0.1 M) of 4-*tert*-butylpyridine at a potential sweep of 0.05 V/s at room temperature. A glassy carbon electrode coated with a thin film of both **T** and **A** was used as the working electrode. Pt and Ag wires were used as the working and reference electrodes, respectively. The electrochemical potential was calibrated against ferrocene/ferrocenium (Fc/Fc^+).

Device Fabrication and Characterization. For the PV device fabrication and its characterization, indium−tin oxide (ITO)-coated glass substrates were cleaned with detergent, deionized water, and accetone and then dried at room temperature. Then the active layers (**A**:PCBM and **T**:PCBM) were spin-coated on ITO substrates from a THF solution at 1500 rpm. We have used a 1:1 weight ratio for both active layers. Finally, the Al electrode was thermally deposited on the top of the photoactive layer to make the sandwiched layer of structure ITO/ photoactive layer/ Al under vacuum ($\sim 10^{-5}$ Torr). The effective area of the devices is about 25 mm^2. For thermal annealing of the photoactive layer, the photoactive layer deposited on the ITO-coated glass was placed on a hot plate at 100 °C for 10 min and then cooled up to room temperature before the final Al electrode was deposited. $J-V$ characteristics were recorded with a Keithley electrometer with a built-in power supply in the dark and under a white-light illumination intensity of 100 mW/cm^2. A 100 W tungsten−halogen lamp was used as a white-light source to illuminate the device. The spectrum of the light source was calibrated with a solar simulator (Newport make). The intensity of the lamp was calibrated and adjusted using an energy meter equipped with a calibrated silicon detector. All of the fabrications and characterizations were performed in an ambient environment.

RESULTS AND DISCUSSION

Synthesis and Characterization. Scheme 1outlines the synthesis of the vinylene compounds **T** and **A**. Particularly, the Heck coupling of the divinyl **1** with **2a** and **2b** in a molar ratio of 1:2 afforded the dialdehydes **3a** and **3b**. The latter reacted with **4** in anhydrous ethanol in the presence of sodium hydroxide to yield the target compounds **T** and **A**. They precipitated a dark-green solid from the reaction mixture in moderate yields (54−57%). Both compounds were readily soluble in common organic solvents such as THF, chloroform, and dichloromethane because of the hexyloxy side chains. Even though the compounds are monomers, thin films of them could be obtained from their solutions by spin-casting.

Structural characterization of the compounds **3a** and **3b** as well as **T** and **A** was performed by FT-IR and ^1H NMR spectroscopy as well as elemental analysis. Compounds **T** and **A** showed characteristic absorption bands, which for **T** appeared at 3080 (aromatic C−H stretching), 1606, 1492, 1448 (C═C aromatic ring stretching band), 2952, 2924, 2866 (C−H stretching of hexyloxy groups), 2154 (cyano group), 1524, 1346 (nitro groups), 1288, 1106 (ether bond), and 966 cm^{-1} (*trans*-olefinic bond). Besides the absorptions at these spectral regions, compound **A** displayed bands at 754 and 736 cm^{-1} associated with the anthracene moiety.

The ^1H NMR spectra of **T** and **A** displayed characteristic upfield signals at ~8.10 (aromatic ortho to nitro group) and ~7.80 ppm (olefinic of the cyano-substituted vinylene bond), while the other olefinic signal resonated at ~7.30 ppm. The elemental analysis shows that the content of carbon, hydrogen, and nitrogen is slightly different from that expected. This indicates that compounds **T** and **A** are not absolutely pure.

The compounds displayed moderate thermal stability, which was evaluated by TGA. No weight loss was observed up to about 270 °C, while the decomposition temperature (T_d) and the char yield (Y_c) at 800 °C were 370−400 °C and 52−70%, respectively (Table 1). **A** was more thermally stable than **T** and showed a slightly higher glass transition

Scheme 1. Synthesis of Compounds T and A

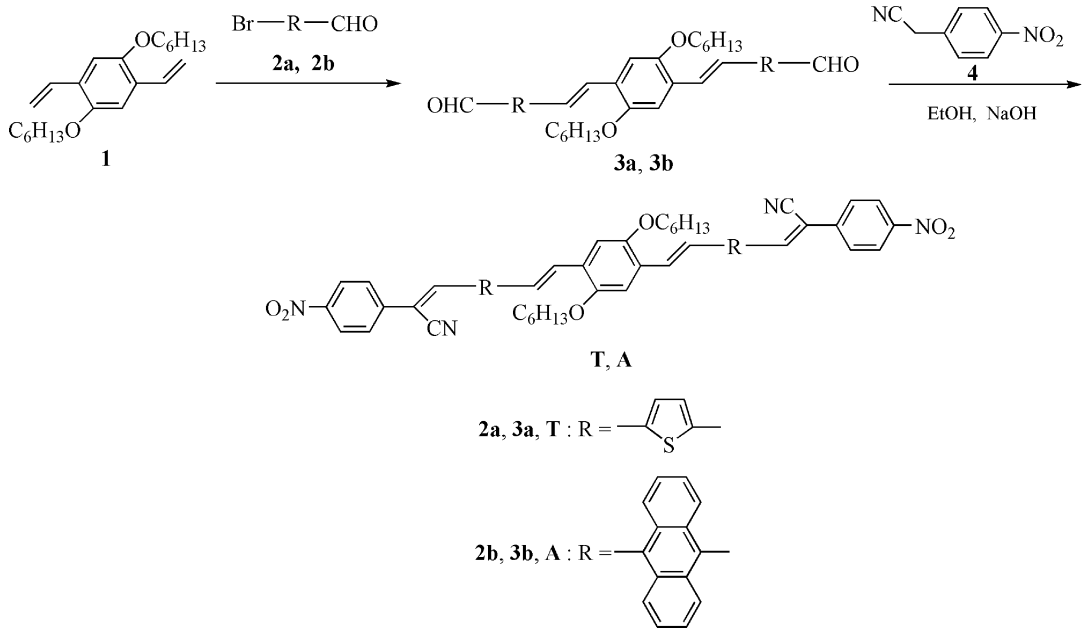

Table 1. Thermal and Optical Properties of Compounds T and A

	T	A
T_d[a] (°C)	370	400
Y_c[b] (%)	52	70
T_g[c]	37	46
$\lambda_{a,max}$[d] in solution (nm)	327, 472, *645*	385, 478, *647*
$\lambda_{a,max}$[d] in a thin film (nm)	334, 471, *637*	383, 476, *630*
E_g^{opt}[e]	1.70 eV (732 nm)[f]	1.71 eV (724 nm)[f]

[a] Decomposition temperature corresponding to 5% weight loss in N_2 determined by TGA. [b] Char yield at 800 °C in N_2 determined by TGA. [c] Glass transition temperature determined by TMA. [d] $\lambda_{a,max}$: absorption maximum from the UV–vis spectra in a THF solution or in a thin film. [e] E_g: optical band gap calculated from the onset of thin-film absorption. [f] Numbers in parentheses indicate the onset of thin-film absorption. Numbers in italics indicate the longer-wavelength absorption maximum.

temperature, which was evaluated by TMA. The relatively high fraction of aliphatic moieties in these molecules suppressed their thermal stability and rigidity.

Photophysical Properties. The UV–vis absorption spectra in a dilute (10^{-5}M) THF solution and a thin film of the synthesized compounds **T** and **A** are shown in Figure 1. Table 1 summarizes all of the photophysical characteristics of the compounds.

T showed three absorption maxima ($\lambda_{a,max}$) around 630, 475, and 640 nm in both the solution and thin film. Likewise, **A** displayed $\lambda_{a,max}$ at about 380, 475, and 640 nm. The two shorter-wavelength absorption peaks, below 500 nm, appeared as shoulders in **T**, while they were more pronounced in **A**. The longer-wavelength $\lambda_{a,max}$ was similar for both compounds in the solution and thin film and located at ~640 nm. Generally, the absorptions of the compounds were broad and extended from 300 up to ~750 nm, which is desirable for PV applications. However, their absorptions were reduced at the range around 550 nm, as seen in Figure 1.

The thin-film absorption onset was located at 732 and 724 nm, which correspond to optical band gaps (E_g^{opt}) of 1.70 and 1.71 eV for **T** and **A**, respectively. These values of E_g^{opt} are significantly lower than that (2.10 eV) of 2-methoxy-5-(2′-ethylhexyloxy)-1,4-phenylenevinylene (MEH-PPV) (52). This suggests a higher intramolecular charge transfer in **T** and **A** than MEH-PPV.

In general, the compounds **T** and **A** were almost equivalent from the optical point of view because they displayed similar photophysical characteristics (Table 1). This supports the theory that the replacement of the thiophene ring with anthracene did not influence considerably the optical properties of the compounds.

PV Properties of Compounds T and A. Parts a and b of Figure 2 show the $J-V$ characteristics of the devices based on **T** and **A** in the dark as well as under illumination of intensity 100 mW/cm^2. The $J-V$ characteristics of both devices in the dark show a rectification effect. Because the work function of ITO (4.8 eV) is very close to that of the HOMO level (−5.0 eV) of both **T** and **A**, it behaves as an ohmic contact for hole injection from ITO into the HOMO level of the compounds. However, the LUMO level (−3.2 eV) of both compounds is far from the work function of Al (4.1 eV) and forms a Schottky barrier for electron injection from Al into the LUMO level of the compounds. Therefore, the rectification is due to the formation of a Schottky barrier at the Al–organic compound interface. The alignment of energy levels of ITO, compound **A**, and Al is shown in the inset of Figure 3. We conclude that both compounds **T** and **A** behave as p-type organic semiconductors (donors) and the devices using these compounds are regarded as hole-dominating devices.

We have estimated the hole mobility of compounds **T** and **A** approximately by the space-charge-limited-current (SCLC) method (53). The $J-V$ of the ITO/compound **A**/Al in the dark

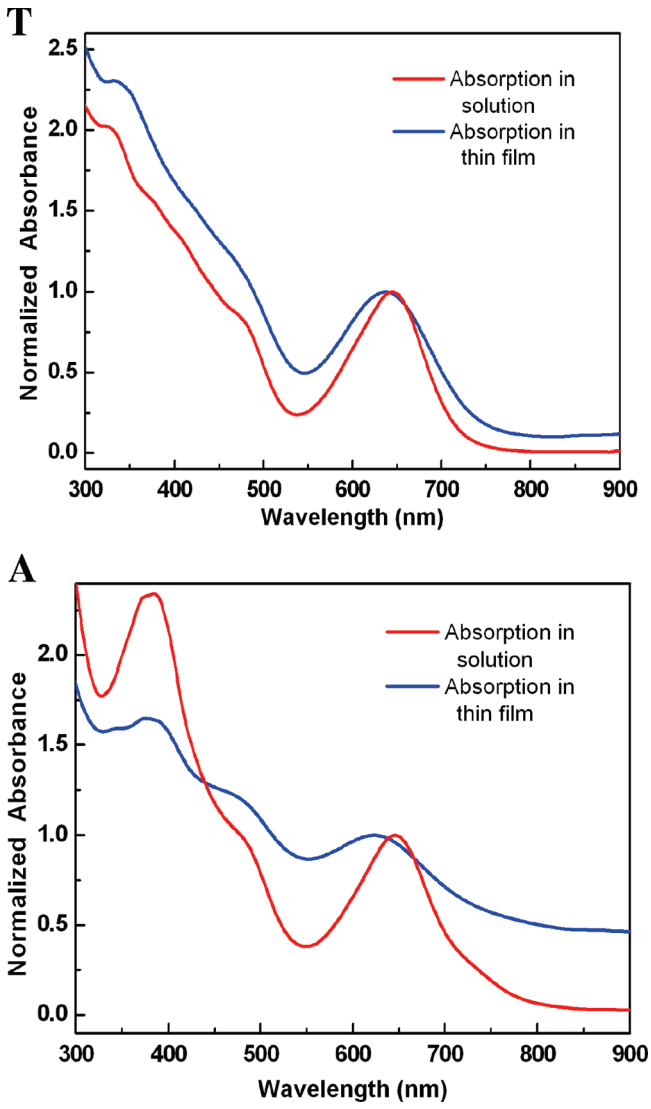

FIGURE 1. Normalized UV−vis absorption spectra in a THF solution and a thin film of compounds T (top) and A (bottom).

on a log− log scale is shown in Figure 3. It can be seen that, in the low-voltage region, log J is linearly dependent on log V with a slope of unity. In the relatively high-voltage region, log J can also be fitted to be linearly dependent on log V and the slope is 2. The $J-V$ curve in this region corresponds to the SCLC behavior. We estimated the hole mobility of compounds **A** and **T** according to equation

$$J = \frac{9}{8}\varepsilon_r \varepsilon_0 \mu_h \frac{(V - V_{bi})^2}{d^3}$$

where V is the applied voltage, J is the current density, ε_r and ε_0 are the relative dielectric constant and permittivity of free space (8.85×10^{-12} F/m), respectively, μ_h is the hole mobility, and d is the thickness of the organic layer. Here we fit ε_r as 3.5 and V_{bi} as 0.7 V, which is determined by the difference in the work function of the electrodes. The hole mobility is in the range of 10^{-5} cm^2/(V s), which is lower than that for P3HT [10^{-3} cm^2/(V s)] (54, 55).

The PV parameters of the device estimated from the $J-V$ characteristics under illumination are complied in Table 2. It is observed that the open-circuit voltage of the device is quite good but the short-circuit current is of the order of microamperes per centimeters squared that decreases the PCE. The low PCE is attributed to the loss of excitons during their transportation because of small exciton diffusion lengths, toward the interface, before dissociation into free carriers. The low value of the hole mobility is also responsible for the low short-circuit photocurrent. However, these materials can be used as BHJ because of the low band gap enhancing the light-harvesting properties in comparison to P3HT.

PV Properties of Compounds T and A Blended with PCBM. The energy levels for HOMO and LUMO of compounds **A**, **T**, and PCBM were obtained by cyclic voltammetry with the method described by Bredas et al. (56). The values of the LUMO and HOMO levels of the compounds **A**, **T**, and PCBM are complied in Table 3. Because the crucial factor for the efficient photoinduced charge transfer in BHJ is the difference between the LUMO level of the donor and acceptor components used in the bulk photoactive layer, this difference should be larger than that of the exciton binding energy, i.e., 0.3 eV (4). The difference in the LUMO levels of PCBM (acceptor) and compound **A** or **T** is more than this. Therefore, the combination of PCBM and compound **A** or **T** is suitable for the photoactive layer to be used in a BHJ PV device.

The $J-V$ characteristics of the ITO/**T**:PCBM/Al and ITO/**A**:PCBM/Al devices in the dark are shown in Figure 4. As can be seen from these figures, the $J-V$ characteristics in the dark of both devices show three distinct regions: (i) a linear region in reverse-bias and low forward-bias voltages, where the current is limited by shunt resistance (R_{sh}), (ii) an exponential region in the intermediate forward-bias voltages, where the current is controlled by the diode, and (iii) a second linear region, where at high forward-bias voltages the current is limited by serial resistance (R_s).

The linearity in the intermediate region of $J-V$ characteristics in both devices in a semilogarthimic representation indicates an exponential relationship between the current and the voltage.

In BHJ devices, the exponential behavior in the $J-V$ characteristics depends upon the properties of the two materials involved in the active layer. The shape of the $J-V$ characteristics in this region depends upon two parameters, i.e., the diode ideality factor (n) and the reverse saturation current (J_o), which is expressed as $J_o \sim \exp(-E_{da}/kT)$, where E_{da} is a parameter analogous to the energy band gap of the conventional semiconductor. The ideality factor gives information about the recombination and shape of the interfaces, i.e., the morphology of the BHJ (57). We have estimated the value of E_{da} from the slope of log(J_o) as a function of $1/T$ and found the value of E_{da} for compound **A** to be about 0.94 eV. This value is less than the band gap of both **A** and PCBM but very close to the energy difference between the HOMO level of **A** and the LUMO level of PCBM. This also indicates the formation of a BHJ, which acts as a single photoactive layer.

Parts a and b of Figure 5 show the $J-V$ characteristics of the devices under illumination of intensity 100 mW/cm^2. The

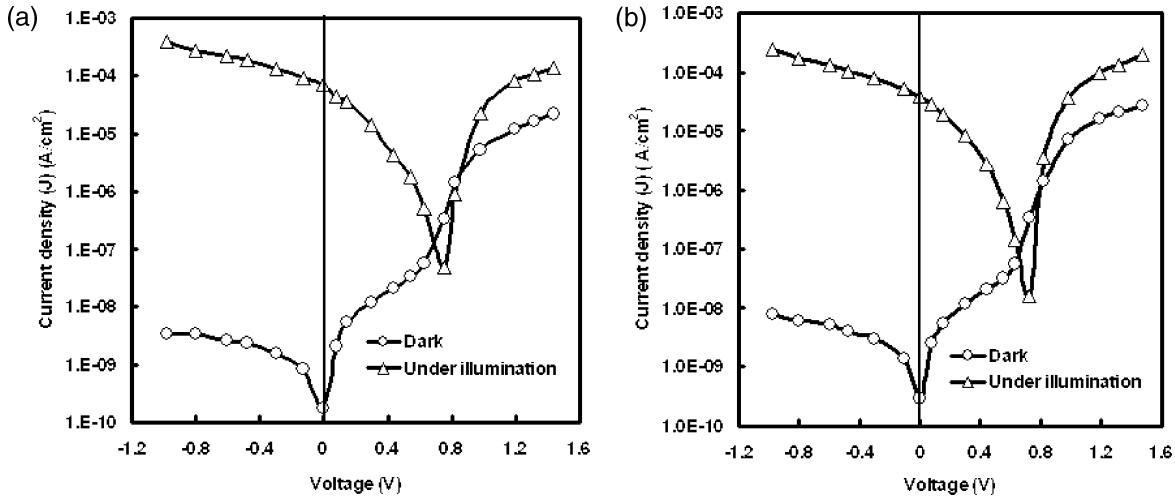

FIGURE 2. (a, left) $J-V$ characteristics of an ITO/compound A/Al device in the dark and under illumination. (b, right) $J-V$ characteristics of an ITO/compound T/Al device in the dark and under illumination.

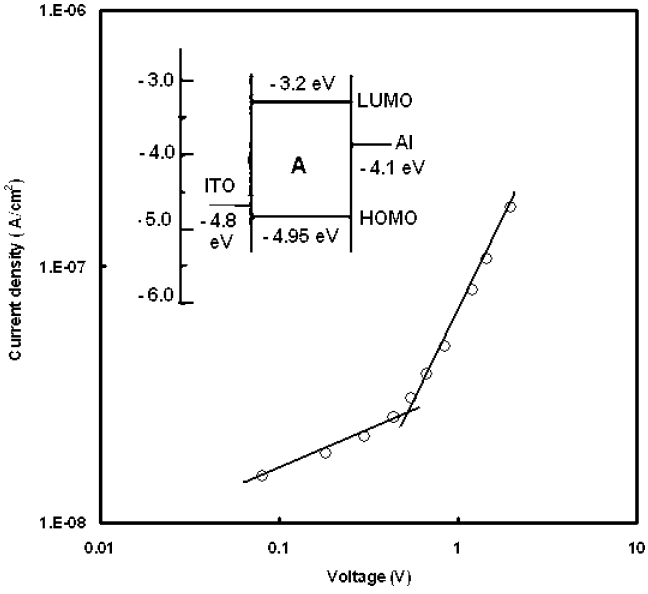

FIGURE 3. $J-V$ curves in the dark of an ITO/compound A/Al device in a log−log plot. The inset is the alignment of the energy levels of compound A and the electrodes.

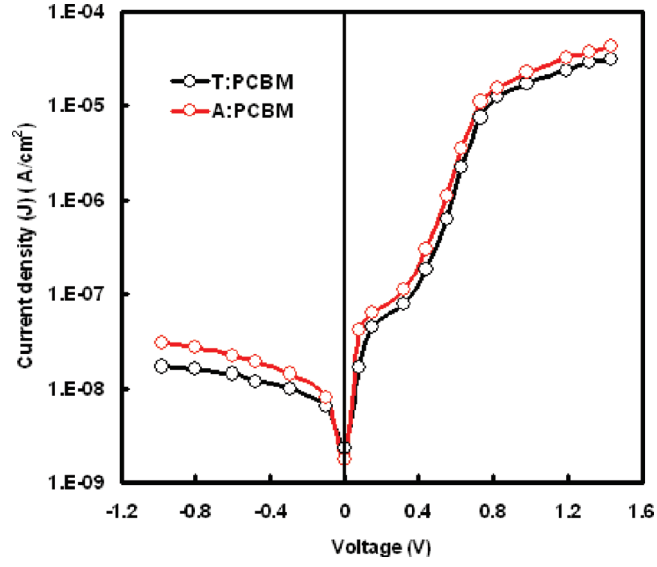

FIGURE 4. $J-V$ characteristics of the devices in the dark at room temperature.

Table 2. PV Parameters of ITO/Compound A/Al and ITO/Compound T/Al Devices

device	short-circuit current (J_{sc}, mA/cm^2)	open-circuit voltage (V_{oc}, V)	fill factor (FF)	PCE (η, %)
ITO/compound **A**/Al	0.072	0.76	0.34	0.019
ITO/compound **T**/Al	0.056	0.73	0.31	0.013

Table 3. HOMO and LUMO Levels of Compounds A, T, and PCBM

material	HOMO (eV)	LUMO (eV)
PCBM	−6.2	−3.9
compound **A**	−4.95	−3.2
compound **T**	−4.83	−3.1

PV parameters of both devices are compiled in Table 4. The values of the PCEs of both devices are more than those obtained for the devices fabricated with compounds **A** and **T**. This indicates that a BHJ is formed in the blend that increases the interfacial interface between the donor and acceptor.

The $J-V$ curves of the devices fabricated with annealed photoactive layers are also shown in Figure 5a,b. The open-circuit voltage decreases slightly upon use of a thermally annealed blend layer, whereas both the short-circuit current and fill factor increase upon thermal annealing. As a result, PCE increases. In the organic solar cells, the product of the charge-carrier lifetime and mobility of charge carriers determines the fill factor (58). Therefore, the enhanced J_{sc} and FF indicate an enhanced carrier transport, which may be attributable to the formation of large donor crystalline domains in the active layer induced by thermal annealing.

It is also found that the thickness of the blend film is decreased from 100 to 85 nm upon thermal annealing. This means that the molecular packing density of the as-cast film is low. Therefore, all molecular interactions between the donor domain, PCBM, and donor:PCBM domain are insufficient. Thermal annealing of the blend leads to an increase

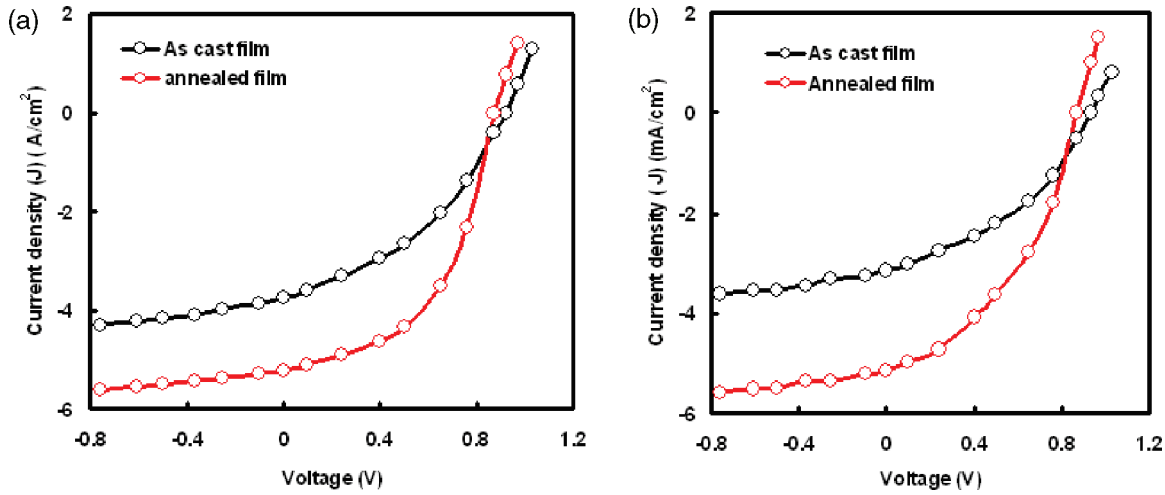

FIGURE 5. (a) $J-V$ characteristics of an ITO/T:PCBM/Al device under illumination using as-cast and annealed photoactive thin-film layers. (b) $J-V$ characteristics of an ITO/A:PCBM/Al device under illumination using as-cast and annealed photoactive thin-film layers.

Table 4. PV Parameters of the BHJ Devices Fabricated from As-Cast and Annealed Photoactive Layers

device	short-circuit current (J_{sc}, mA/cm^2)	open-circuit voltage (V_{oc}, V)	fill factor (FF)	PCE (η, %)
ITO/**A**:PCBM/Al	3.75	0.92	0.48	1.66
ITO/**A**:PCBM (annealed)/Al	5.30	0.87	0.54	2.49
ITO/**T**:PCBM/Al	3.14	0.94	0.46	1.36
ITO/**T**:PCBM (annealed)/Al	5.16	0.85	0.53	2.33

in the packing density; i.e., the distance between all molecules is narrowed and, therefore, the efficiencies of exciton dissociation and charge transport are improved. The enhancement in the photocurrent may also be attributed to the balanced charge transport in the device due to the enhanced hole mobility in compound **A** or **T** and increases light harvesting by the annealed blend. The combined effect of the above mechanisms results in an improvement in the overall PCE upon thermal annealing of the blend.

CONCLUSIONS

Two new *p*-phenylenevinylene compounds, **T** and **A**, were synthesized by a simple two-step synthetic route. The hexyloxy side groups, which were attached to the central phenylene, enhanced the solubility of the compounds but suppressed their thermal stability and rigidity. These two small molecules had D−A architecture and allowed intramolecular energy transfer, which reduced their optical band gap. Both compounds showed broad absorption with a longer-wavelength absorption maximum of around 640 nm and optical band gaps of 1.70−1.71 eV. The $J-V$ characteristics of the devices in the dark sandwiched between Al and ITO electrodes suggest that both compounds **T** and **A** behave as a p-type organic semiconductor (donor). The PCEs of the devices based on **A**:PCBM and **T**:PCBM are about 1.66% and 1.36%, respectively, which is further improved up to 2.49% and 2.33%, using the thermally annealed blended layers.

Acknowledgment. Authors G.D.S., P.B., and P.S. are thankful to CSIR for financial assistance throughout the project. We are also thankful to Dr. M. S. Roy for providing the facility for the cyclic voltammetry measurements.

Supporting Information Available: FT-IR spectra, ^{1}H NMR spectra, and TGA and TMA thermograms of compounds **T** and **A**. This material is available free of charge via the Internet at http://pubs.acs.org.

REFERENCES AND NOTES

(1) Shaheen, S. E.; Ginley, D. S.; Jabour, G. E. *MRS Bull.* **2005**, *30*, 10–19.
(2) Sariciftci, N. S.; Smilowitz, L.; Heeger, A. J.; Wudl, F. *Science* **1992**, *258*, 1474–1476.
(3) (a) Yu, G.; Gao, J.; Hummelen, C. J.; Wudl, F.; Heeger, A. J. *Science* **1995**, *270*, 1789–1791. (b) Brabec, C. J.; Sariciftci, N. S.; Hummelen, J. C. *Adv. Funct. Mater.* **2001**, *11*, 15–26. (c) Hoppe, H.; Sariciftci, N. S. *J. Mater. Chem.* **2006**, *16*, 45–61. (d) Günes, S.; Neugebauer, H.; Sariciftci, N. S. *Chem. Rev.* **2007**, *107*, 1324–1338. (e) Thompson, B. C.; Fréchet, J. M. J. *Angew. Chem., Int. Ed.* **2008**, *47*, 58–77.
(4) Li, G.; Shrotriya, V.; Huang, J.; Yao, Y.; Moriarity, T.; Emery, K.; Yang, Y. *Nat. Mater.* **2005**, *4*, 864–868.
(5) Cacialli, F.; Chuah, B. S.; Friend, R. H.; Moratti, S. C.; Holmes, A. B. *Synth. Met.* **2000**, *111*, 155–158.
(6) Braun, D.; Heeger, A. J. *Appl. Phys. Lett.* **1991**, *58*, 1982–1984.
(7) Bradley, D. D. C. *Adv. Mater.* **1992**, *4*, 756–758.
(8) Andersson, M. R.; Yu, G.; Heeger, A. J. *Synth. Met.* **1997**, *85*, 1275–1276.
(9) Alem, S.; de Bettignies, R.; Nunzi, J.-M. *Appl. Phys. Lett.* **2004**, *84*, 2178–2180.
(10) Yu, G.; Gao, J.; Hummelen, J. C.; Wudl, F.; Heeger, A. J. *Science* **1995**, *270*, 1789–1791.
(11) Yang, C.; Li, H.; Sun, Q.; Qiao, J.; Li, Y.; Li, Y.; Zhu, D. *Sol. Energy Mater. Sol. Cells* **2004**, *85*, 241–249.
(12) Shi, Q.; Hou, Y.; Lu, J.; Jin, H.; Li, Y.; Li, Y.; Sun, X.; Liu, J. *Chem. Phys. Lett.* **2006**, *425*, 353–355.
(13) Sirimanne, P. M.; Premalal, E. V. A.; Pitigala, P. K. D. D. P.; Tennakone, K. *Sol. Energy Mater. Sol. Cells* **2006**, *90*, 1673–1679.
(14) Kumar, A.; Bhatnagar, P. K.; Mathur, P. C.; Tada, K.; Onoda, M. *Appl. Surf. Sci.* **2006**, *252*, 3953–3955.
(15) Choi, D. H.; Cho, M. J.; Han, K. I.; Chang, I.-H.; Song, J. S.; Kim, J. H.; Paek, S.-H.; Choi, S.-H. *Synth. Met.* **2006**, *156*, 685–689.
(16) Quan, S.; Teng, F.; Xu, Z.; Qian, L.; Hou, Y.; Wang, Y.; Xu, X. *Eur. Polym. J.* **2005**, *42*, 228–233.
(17) Biswas, A. K.; Tripathi, A.; Singh, S.; Mohapatra, Y. N. *Synth. Met.* **2005**, *155*, 340–343.
(18) Mirzov, O.; Pullerits, T.; Cichos, F.; von Borczyskowski, C.; Scheblykin, I. G. *Chem. Phys. Lett.* **2005**, *408*, 317–321.

(19) Mirzov, O.; Cichos, F.; von Borczyskowski, C.; Scheblykin, I. *J. Lumin.* **2005**, *112*, 353–356.
(20) Mirzov, O.; Cichos, F.; von Borczyskowski, C.; Scheblykin, I. G. *Chem. Phys. Lett.* **2004**, *386*, 286–290.
(21) Halls, J. J. M.; Walsh, C. A.; Greenham, N. C.; Marseglla, E. A.; Friend, R. H.; Moratti, S. C.; Holmes, A. B. *Nature* **1995**, *376*, 498–500.
(22) Liu, M. S.; Jiang, X. Z.; Liu, S.; Herguth, P.; Jen, A. K.-Y. *Macromolecules* **2002**, *35*, 3532–3538.
(23) Zou, Y.; Hou, J.; Yang, C.; Li, Y. *Macromolecules* **2006**, *39*, 8889–8891.
(24) Greenwald, Y.; Cohen, G.; Poplawski, J.; Ehrenfreund, E.; Speiser, S.; Davidov, D. *Synth. Met.* **1995**, *69*, 365–366.
(25) Greenwald, Y.; Cohen, G.; Poplawski, J.; Ehrenfreund, E.; Speiser, S.; Davidov, D. *J. Am. Chem. Soc.* **1996**, *118*, 2980–2984.
(26) Zotti, G.; Zecchin, S.; Schiavon, G. *Chem. Mater.* **1995**, *7*, 2309–2315.
(27) Reddinger, J. L.; Reynolds, J. R. *Macromolecules* **1997**, *30*, 673–675.
(28) He, Y.; Wang, X.; Zhang, J.; Li, Y. *Macromol. Rapid Commun.* **2009**, *30*, 45–51.
(29) Cutler, C. A.; Burrell, A. K.; Collis, G. E.; Dastoor, P. C.; Officer, D. L.; Too, C. O.; Wallace, G. G. *Synth. Met.* **2001**, *123*, 225–237.
(30) Kim, H.-S.; Kim, C.-H.; Ha, C.-S.; Lee, J.-K. *Synth. Met.* **2001**, *117*, 289–291.
(31) Hou, J.; Huo, L.; He, C.; Yang, C.; Li, Y. *Macromolecules* **2006**, *39*, 594–603.
(32) Valentini, L.; Bagnis, D.; Marrocchi, A.; Seri, M.; Taticchi, A.; Kenny, J. M. *Chem. Mater.* **2008**, *20*, 32–34.
(33) Vellis, P. D.; Mikroyannidis, J. A.; Bagnis, D.; Valentini, L.; Kenny, J. M. *J. Appl. Polym. Sci.* **2009**, *113*, 1173−1181.
(34) Lloyd, M. T.; Anthony, J. E.; Malliaras, G. G. *Mater. Today* **2007**, *10*, 34–41.
(35) Xue, L.; He, J.; Gu, X.; Yang, Z.; Xu, B.; Tian, W. *J. Phys. Chem. C* ASAP.
(36) Wang, S.; Mayo, E. I.; Perez, M. D.; Griffe, L.; Wei, G.; Djurovich, P. I.; Forrest, S. R.; Thompson, M. E. *Appl. Phys. Lett.* **2009**, *94*, 233304/1–233304/3.
(37) Silvestri, F.; Irwin, M. D.; Beverina, L.; Facchetti, A.; Pagani, G. A.; Marks, T. J. *J. Am. Chem. Soc.* **2008**, *130*, 17640–17641.
(38) Taima, T.; Sakai, J.; Yamanari, T.; Saito, K. *Sol. Energy Mater. Sol. Cells* **2009**, *93*, 742–745.
(39) Aich, R.; Ratier, B.; Tran-van, F.; Goubard, F.; Chevrot, C. *Thin Solid Films* **2008**, *516*, 7171–7175.
(40) Tamayo, A. B.; Dang, X.-D.; Walker, B.; Seo, J.; Kent, T.; Nguyen, T.-Q. *Appl. Phys. Lett.* **2009**, *94*, 103301/1–103301/3.
(41) Peet, J.; Tamayo, A. B.; Dang, X.-D.; Seo, J. H.; Nguyen, T.-Q. *Appl. Phys. Lett.* **2008**, *93*, 163306/1–163306/3.
(42) Schubert, M.; Yin, C.; Castellani, M.; Bange, S.; Tam, T. L.; Sellinger, A.; Hörhold, H.-H.; Kietzke, T.; Neher, D. *J. Chem. Phys.* **2009**, *130*, 094703/1–094703/3.
(43) Ooi, Z. E.; Tam, T. L.; Shin, R. Y. C.; Chen, Z. K.; Kietzke, T.; Sellinger, A.; Baumgarten, M.; Mullen, K.; deMello, J. C. *J. Mater. Chem.* **2008**, *18*, 4619–4622.
(44) He, C.; He, Q.; Yi, Y.; Wu, G.; Bai, F.; Shuai, Z.; Li, Y. *J. Mater. Chem.* **2008**, *18*, 4085–4090.
(45) Wu, G.; Zhao, G.; He, C.; Zhang, J.; He, Q.; Chen, X.; Li, Y. *Sol. Energy Mater. Sol. Cells* **2009**, *93*, 108–113.
(46) Zhao, G.; Wu, G.; He, C.; Bai, F.-Q.; Xi, H.; Zhang, H.-X.; Li, Y. *J. Phys. Chem. C* **2009**, *113*, 2636–2642.
(47) He, C.; He, Q.; Yang, X.; Wu, G.; Yang, C.; Bai, F.; Shuai, Z.; Wang, L.; Li, Y. *J. Phys. Chem. C* **2007**, *111*, 8661–8666.
(48) He, C.; He, Q.; He, Y.; Li, Y.; Bai, F.; Yang, C.; Ding, Y.; Wang, L.; Ye, J. *Sol. Energy Mater. Sol. Cells* **2006**, *90*, 1815–1827.
(49) McKean, D. R.; Parrinello, G.; Renaldo, A. F.; Stille, J. K. *J. Org. Chem.* **1987**, *52*, 422–424.
(50) Peng, Q.; Li, M.; Tang, X.; Lu, S.; Peng, J.; Cao, Y. *J. Polym. Sci., Part A: Polym. Chem.* **2007**, *45*, 1632–1640.
(51) Babasinian, V. S. *Organic Syntheses*, Collect. Vol. 2, p 466 (1943); Vol. 14, p 76 (1934).
(52) Li, X.; Zhang, Y.; Yang, R.; Huang, J.; Yang, W.; Cao, Y. *J. Polym. Sci., Part A: Polym. Chem.* **2005**, *43*, 2325–2336.
(53) Blom, P. W. M.; de Jong, M. J. M.; van Munster, M. G. *Phys. Rev. B* **1997**, *55*, R656−R659.
(54) Pivrikas, A.; Juska, G.; Mozer, A. J.; Scharber, M.; Karlauskas, A.; Sariciftci, N. S.; Stubb, H.; Osterbacka, R. *Phys. Rev. Lett.* **2005**, *94*, 176806/1–176806/4.
(55) Bao, Z.; Dodabalapur, A.; Lovinger, A. *Appl. Phys. Lett.* **1996**, *69*, 4108–4110.
(56) Bredas, J. L.; Silbey, R.; Boudreux, D. S.; Chance, R. R. *J. Am. Chem. Soc.* **1983**, *105*, 6555–6559.
(57) Waldauf, C.; Schilinsky, P.; Hauch, J.; Brabec, C. J. *Thin Solid Films* **2004**, *451−452*, 503–507.
(58) *Organic Photovoltaics Mechanisms, Materials, and Devices*; Sun, S. S., Sariciftci, N. S., Eds.; CRC Press: Boca Raton, FL, 2005.

AM900270S